phys. stat. sol. (b) 76, K15 (1976)

Subject classification: 6 and 20.1; 22

Physikalisches Institut der Universität Würzburg

Infra red-Active Lattice Vibrations in $SnSe_2$

By

H. KÖHLER and C.R. BECKER

$SnSe_2$ is a layer-type semiconductor having the CdI_2 crystal structure whose symmetry corresponds to the D^3_{3d} space group. It consists of layers of tin atoms sandwiched between two layers of selenium atoms in a hexagonally closest packing arrangement. This unit of three layers is periodically repeated along the c axis; - Se] - [Se-Sn-Se] -[Se-Sn. Within this unit Sn is covalently bound (sp^3d^2) to six Se atoms in an octahedral configuration, where Sn occupies the centre of inversion in the unit cell. Bonding between threefold layers is thought to be due to van der Waals forces between filled s electron shells of Se atoms in adjoining layers.

A Wigner-Seitz cell may be constructed, containing one tin and two selenium atoms. As a basis for the lattice vibrations the three atoms on a straight line may be chosen to demonstrate the normal modes in the centre of the Brillouin zone (Fig. 1).

The irreducible representation of all the lattice modes at Γ (centre of the Brillouin zone) is

$$\Gamma = A_{1g} + E_g + 2A_{2u} + 2E_u \,. \tag{1}$$

As indicated in Fig. 1, Γ is composed of two acoustical, two infrared- and two Raman-active modes. Because of inversion symmetry the non-acoustical modes are either Raman- or infrared-active at q = 0. Both Raman frequencies were observed earlier in the xx and xy pola-

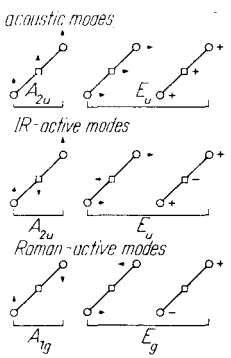

Fig. 1. Schematic representation of possible movements of the atoms (○ Se; □ Sn) within the chosen basis relative to each other for the 3N = 9 different modes. Plus and minus signs correspond to movements normal to the drawing plane

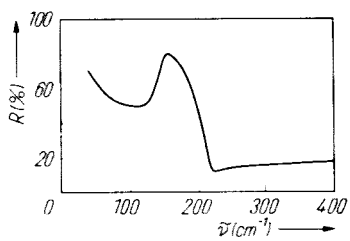

Fig. 2

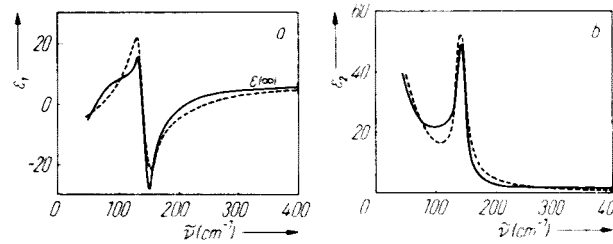

Fig. 3

Fig. 2. Reflectivity of a $SnSe_2$ sample in the polarization configuration $\vec{E} \perp \vec{c}$ ($\vec{c}$, the trigonal axis, is normal to the reflecting surface) at 15 K between 40 and 400 cm^{-1}

Fig. 3. a) and b) Real (ε_1) and imaginary (ε_2) part of the dielectric constant ($\vec{E} \perp \vec{c}$) obtained from Kramers-Kronig analysis (solid curves) of the reflectivity curve in Fig. 2 and by numerical calculations (dashed curves) on the basis of a classical oscillator taking into consideration the influence of free carriers

rization configurations (1). The two infrared-active modes, A_{2u} and E_u, should influence the FIR optical properties for $\vec{E} \parallel \vec{c}$ and $\vec{E} \perp \vec{c}$, respectively.

Free carrier optical effects were investigated earlier at higher frequencies (2), (3). Using a Polytec FIR 30 Fourier spectrometer we were able to extend the spectral region down to about 40 cm^{-1} wave numbers. The crystals were grown by a vertical Bridgman technique. The samples were cut with a corundum saw and subsequently cleaved in order to obtain surfaces perpendicular to the c-axis (polarization $\vec{E} \perp \vec{c}$). Because the crystals are very soft, cutting and polishing did not yield optical surfaces parallel to the c-axis of sufficiently high quality, to allow investigations for the polarization configuration $\vec{E} \parallel \vec{c}$.

In Fig. 2 the reflectivity of one $SnSe_2$ sample is shown between 40 and 400 cm^{-1} at about 15 K. The results are essentially unchanged at 300 K. Above about 125 cm^{-1} the change in reflectivity is caused by the E_u mode, while at lower wave numbers the influence of free carriers becomes more significant. The solid curves in Fig. 3a and b were obtained by Kramers-Kronig analysis for the real (ε_1) and the imaginary (ε_2) part of the dielectric constant, the dashed curves for ε_1 and ε_2 were calculated by means of a classical oscillator fit, taking into account the influence of the free

carriers with the normal Drude formalism. As can be seen, the agreement is not very good, and in particular the non-symmetric shape of the ε_2 curve near $\tilde{\nu}_t$ = = 142 cm^{-1} could not be reproduced. For the same reason, the ε_1 curves do not agree near $\tilde{\nu}_t$. We did not attempt to look for physically realistic arguments in order to explain the deviations, because the sample quality was far from perfect. Therefore, we have tried to reach a maximum average agreement in the ε_1 and ε_2 curves, in order to give the best possible value for the oscillator frequency and static dielectric constant. The parameters which were either employed or determined are as follows: $\varepsilon(\infty) = 7$ (2), the electron concentration $N = 1.3 \times 10^{18}$ cm^{-3}, the effective electron mass $m^* = 0.4\ m_o$ (2), the electron relaxation time $\tau = 4.5 \times 10^{-14}$ s (deduced from an electron mobility of 200 cm^2/Vs), the contribution of the lattice oscillator to the dielectric constant $\Delta\varepsilon = 6.1$, the oscillator frequency $\tilde{\nu}_t = 142$ cm^{-1}, and the ε_2 half-width $2\Delta\tilde{\nu} = 20$ cm^{-1}.

Hence a static dielectric constant, $\varepsilon(0) = 13 \pm 10\%$, may be derived for the polarization $\vec{E} \perp \vec{c}$. The Lyddane-Sachs-Teller relation, $\tilde{\nu}_l = (\varepsilon(0)/\varepsilon(\infty))^{1/2}\, \tilde{\nu}_t$, yields 194 cm^{-1} for $\tilde{\nu}_l$, which is modified in the experimental results by the influence of the free carriers. Comparison of the absorption constant of the lattice oscillator at high frequencies above 1000 cm^{-1} with the data of the free carrier absorption shows the dominating influence of the electronic properties and hence is a confirmation of the conclusions in (2).

The financial support of the Deutsche Forschungsgemeinschaft is acknowledged.

References

(1) O.P. AGNIHOTRI, A.K. GARG, and H.K. SEHGAL, Solid State Commun. 17, 1537 (1975).

(2) P.A. LEE and G. SAID, J. Phys. D, Ser. 2, 1, 837 (1968).

(3) B.L. EVANS and R.A. HAZELWOOD, J. Phys. D, Ser. 2, 2, 1507 (1969).

(Received May 7, 1976)